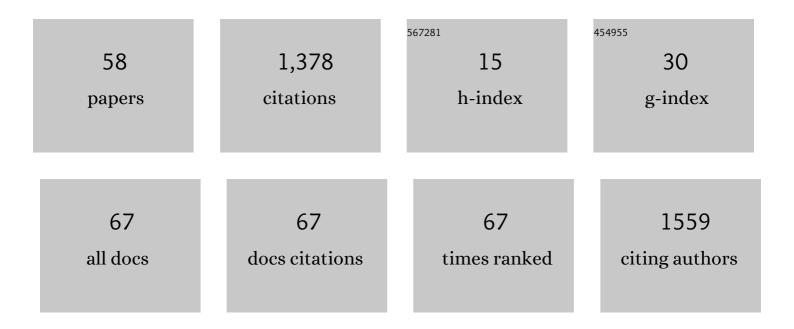
List of Publications by Year in descending order

Source: https://exaly.com/author-pdf/5407951/publications.pdf Version: 2024-02-01



#	Article	IF	CITATIONS
1	Serum Selenium Levels in Glaucoma: a Pilot Study. Klinische Monatsblatter Fur Augenheilkunde, 2022, 239, 326-330.	0.5	1
2	Long COVID: Association of Functional Autoantibodies against G-Protein-Coupled Receptors with an Impaired Retinal Microcirculation. International Journal of Molecular Sciences, 2022, 23, 7209.	4.1	39
3	Two-Year Follow-Up: Therapeutic Success with Respect to Axial Length of Stand-Alone Xen45 Gel Stent Implantation and Combined Procedures. Klinische Monatsblatter Fur Augenheilkunde, 2021, 238, 1240-1247.	0.5	1
4	Influence of Mitomycin C on the Therapeutic Success of Stand-Alone Xen45 Gel Stents and Its Combination with Cataract Surgery in Open-Angle Glaucoma Patients. Klinische Monatsblatter Fur Augenheilkunde, 2021, 238, 861-867.	0.5	3
5	Summation of Temporal L-Cone- and M-Cone-Contrast in the Magno- and Parvocellular Retino-Geniculate Systems in Glaucoma. , 2021, 62, 17.		4
6	Agonistic β2-Adrenergic Receptor Autoantibodies Characterize the Aqueous Humor of Patients With Primary and Secondary Open-Angle Glaucoma. Frontiers in Immunology, 2021, 12, 550236.	4.8	5
7	Agonistic autoantibodies against ß2-adrenergic receptor influence retinal microcirculation in glaucoma suspects and patients. PLoS ONE, 2021, 16, e0249202.	2.5	8
8	Erlanger Glaucoma Registry: Effect of a Long-Term Therapy with Statins and Acetyl Salicylic Acid on Glaucoma Conversion and Progression. Biology, 2021, 10, 538.	2.8	6
9	Extended Ganglion Cell Layer Thickness Deviation Maps With OCT in Glaucoma Diagnosis. Frontiers in Medicine, 2021, 8, 684676.	2.6	1
10	Responses of Postreceptoral Pathways Elicited by L- and M-Cone Isolating ON- and OFF-Electroretinograms in Glaucoma Patients. , 2021, 62, 14.		0
11	Inhibitory and Agonistic Autoantibodies Directed Against the β2-Adrenergic Receptor in Pseudoexfoliation Syndrome and Glaucoma. Frontiers in Neuroscience, 2021, 15, 676579.	2.8	5
12	Glaucoma classification in 3 x 3 mm en face macular scans using deep learning in different plexus. Biomedical Optics Express, 2021, 12, 7434.	2.9	9
13	Case Report: Neutralization of Autoantibodies Targeting G-Protein-Coupled Receptors Improves Capillary Impairment and Fatigue Symptoms After COVID-19 Infection. Frontiers in Medicine, 2021, 8, 754667.	2.6	38
14	Blue–Yellow VEP with Projector-Stimulation in Glaucoma. Graefe's Archive for Clinical and Experimental Ophthalmology, 2021, , 1.	1.9	2
15	Five-Year Long-Term Follow-Up of Selective Laser Trabeculoplasty in Open-Angle Glaucoma. Klinische Monatsblatter Fur Augenheilkunde, 2021, , .	0.5	0
16	Germany: Longitudinal analysis of intraocular pressure in healthy eyes. Cogent Medicine, 2020, 7, .	0.7	2
17	Autoantibodies Activating the β2-Adrenergic Receptor Characterize Patients With Primary and Secondary Glaucoma. Frontiers in Immunology, 2019, 10, 2112.	4.8	11
18	In Reply: Precision of Optic Nerve Head and Retinal Nerve Fiber Layer Parameter Measurements by Spectral-domain Optical Coherence Tomography, Methodological Issues on Reproducibility. Journal of Glaucoma, 2018, 27, e95-e100.	1.6	0

#	Article	IF	CITATIONS
19	MIGS: therapeutic success of combined Xen Gel Stent implantation with cataract surgery. Graefe's Archive for Clinical and Experimental Ophthalmology, 2018, 256, 621-625.	1.9	53
20	Precision of Optic Nerve Head and Retinal Nerve Fiber Layer Parameter Measurements by Spectral-domain Optical Coherence Tomography. Journal of Glaucoma, 2018, 27, 407-414.	1.6	17
21	Structural changes of macular inner retinal layers in early normal-tension and high-tension glaucoma by spectral-domain optical coherence tomography. Graefe's Archive for Clinical and Experimental Ophthalmology, 2018, 256, 1245-1256.	1.9	15
22	Predictive Factors for Visual Field Conversion. Journal of Glaucoma, 2018, 27, 157-163.	1.6	2
23	ICE-Syndrome: A Case Report of Implantation of a Microbypass Xen Gel Stent After DMEK Transplantation. Journal of Glaucoma, 2017, 26, e103-e104.	1.6	27
24	Can Glaucomatous Visual Field Progression be Predicted by Structural and Functional Measures?. Journal of Glaucoma, 2017, 26, 373-382.	1.6	13
25	Comparison of Bruch's Membrane Opening Minimum Rim Width and Peripapillary Retinal Nerve Fiber Layer Thickness in Early Glaucoma Assessment. , 2016, 57, OCT575.		82
26	Confocal Laser Scanning Tomography to Predict Visual Field Conversion in Patients With Ocular Hypertension and Early Glaucoma. Journal of Glaucoma, 2016, 25, 371-376.	1.6	8
27	Retinal imaging and axonal degeneration in later onset multiple sclerosis. Journal of the Neurological Sciences, 2016, 370, 1-6.	0.6	2
28	Comparison of frequency doubling and flicker defined form perimetry in early glaucoma. Graefe's Archive for Clinical and Experimental Ophthalmology, 2016, 254, 937-946.	1.9	12
29	The Effect of Long-term Antiglaucomatous Drug Administration on Central Corneal Thickness. Journal of Glaucoma, 2016, 25, 274-280.	1.6	16
30	Baseline Magnetic Resonance Imaging of the Optic Nerve Provides Limited Predictive Information on Short-Term Recovery after Acute Optic Neuritis. PLoS ONE, 2015, 10, e0113961.	2.5	21
31	Short-term fluctuation of intraocular pressure is higher in patients with pseudoexfoliation syndrome despite similar mean intraocular pressure: a retrospective case–control study. Graefe's Archive for Clinical and Experimental Ophthalmology, 2015, 253, 107-114.	1.9	12
32	Predicted and Measured Retinal Nerve Fiber Layer Thickness From Time-Domain Optical Coherence Tomography Compared With Spectral-Domain Optical Coherence Tomography. JAMA Ophthalmology, 2015, 133, 1135.	2.5	8
33	Longitudinal stability of the diurnal rhythm of intraocular pressure in subjects with healthy eyes, ocular hypertension and pigment dispersion syndrome. BMC Ophthalmology, 2014, 14, 122.	1.4	1
34	Perimetric Measurements With Flicker-Defined Form Stimulation in Comparison With Conventional Perimetry and Retinal Nerve Fiber Measurements. , 2014, 55, 2317.		14
35	Thickness related textural properties of retinal nerve fiber layer in color fundus images. Computerized Medical Imaging and Graphics, 2014, 38, 508-516.	5.8	27
36	Glaucoma Diagnostic Performance of GDxVCC and Spectralis OCT on Eyes With Atypical Retardation Pattern. Journal of Glaucoma, 2013, 22, 317-324.	1.6	11

#	Article	IF	CITATIONS
37	Longitudinal Analysis of Progression in Glaucoma Using Spectral-Domain Optical Coherence Tomography. , 2013, 54, 3613.		65
38	Analysis of Visual Appearance of Retinal Nerve Fibers in High Resolution Fundus Images: A Study on Normal Subjects. Computational and Mathematical Methods in Medicine, 2013, 2013, 1-10.	1.3	10
39	An empirical study of algebraic-reconstruction techniques. , 2013, , 111-116.		Ο
40	Combined Evaluation of Frequency Doubling Technology Perimetry and Scanning Laser Ophthalmoscopy for Glaucoma Detection Using Automated Classification. Journal of Glaucoma, 2012, 21, 27-34.	1.6	16
41	On- and off-response ERGs elicited by sawtooth stimuli in normal subjects and glaucoma patients. Documenta Ophthalmologica, 2012, 124, 237-248.	2.2	28
42	Atypical Retardation Patterns in Scanning Laser Polarimetry Are Associated with Low Peripapillary Choroidal Thickness. , 2011, 52, 7523.		4
43	Comparison of Scanning Laser Polarimetry and Optical Coherence Tomography in Quantitative Retinal Nerve Fiber Assessment. Journal of Glaucoma, 2010, 19, 83-94.	1.6	20
44	In Response:. Journal of Glaucoma, 2010, 19, 222-224.	1.6	2
45	Retinal Nerve Fiber Layer Thickness in Normals Measured by Spectral Domain OCT. Journal of Glaucoma, 2010, 19, 475-482.	1.6	178
46	Detection of nerve fiber atrophy in apparently effectively treated papilledema in idiopathic intracranial hypertension. Graefe's Archive for Clinical and Experimental Ophthalmology, 2010, 248, 1787-1793.	1.9	10
47	Morphologic and functional glaucomatous change after occurrence of single or recurrent optic disc hemorrhages. Graefe's Archive for Clinical and Experimental Ophthalmology, 2010, 248, 1683-1684.	1.9	10
48	Correlation between Local Glaucomatous Visual Field Defects and Loss of Nerve Fiber Layer Thickness Measured with Polarimetry and Spectral Domain OCT. , 2009, 50, 1971.		83
49	Influence of Glaucomatous Damage and Optic Disc Size on Glaucoma Detection by Scanning Laser Tomography. Journal of Glaucoma, 2009, 18, 385-389.	1.6	15
50	Visualization of Changes of the Iris Configuration After Peripheral Laser Iridotomy in Primary Melanin Dispersion Syndrome Using Optical Coherence Tomography. Journal of Glaucoma, 2008, 17, 569-570.	1.6	17
51	Association of <i>LOXL1</i> Common Sequence Variants in German and Italian Patients with Pseudoexfoliation Syndrome and Pseudoexfoliation Glaucoma. , 2008, 49, 1459.		114
52	Semiautomatic Detection and Evaluation of Autofluorescent Areas in Retinal Images. Annual International Conference of the IEEE Engineering in Medicine and Biology Society, 2007, 2007, 3327-30.	0.5	2
53	Quantification of Neuroretinal Rim Loss Using Digital Planimetry in Long-term Follow-up of Normals and Patients With Ocular Hypertension. Journal of Glaucoma, 2007, 16, 430-436.	1.6	14
54	Measuring contrast sensitivity in normal subjects with OPTEC® 6500: influence of age and glare. Graefe's Archive for Clinical and Experimental Ophthalmology, 2007, 245, 1805-1814.	1.9	114

#	Article	IF	CITATIONS
55	Influence of optic disc size on parameters of retinal nerve fiber analysis with laser scanning polarimetry. Graefe's Archive for Clinical and Experimental Ophthalmology, 2006, 244, 603-608.	1.9	7
56	Measurement of autofluorescence in the parapapillary atrophic zone in patients with ocular hypertension. Graefe's Archive for Clinical and Experimental Ophthalmology, 2006, 245, 51-58.	1.9	14
57	Automated segmentation of the optic nerve head for diagnosis of glaucoma. Medical Image Analysis, 2005, 9, 297-314.	11.6	143
58	Automated Segmentation of the Optic Nerve Head for Glaucoma Diagnosis. Informatik Aktuell, 2003, , 338-342.	0.6	4